Differentiation of isomeric cresols by silylation in combination with GC-MS analysis

Jiaxiang Xu[a], Guohua Zhu[b], Huarong Zhang[a*], Jinsong Liu[b], Kezhi Jiang[a*]

a. Key Laboratory of Organosilicon Chemistry and Material Technology, Hangzhou Normal University, Hangzhou, 311121, China

b. Zhejiang Province Environmental Monitoring Center, Hangzhou, 310015, China

Address Correspondence to:

Huarong Zhang, Dr., Email: zhanghuaxy99@hznu.edu.cn

Kezhi Jiang, A.P., Dr., Email: jiangkezhi@hznu.edu.cn

Rationale: *m*-Cresol is listed as the priority controlled contamination in many countries, but it is very difficult to accurately determine isomeric cresols due to the incomplete chromatographic separation of them on a commercially available chromatographic column and their nearly identical mass spectra.

Methods: Silylation of the isomeric cresols was carried out by treatment with *N*-methyl-*N*-(trimethylsilyl)trifluoro acetamide (MSTFA). The formed trimethyl(tolyloxy)silanes were analyzed by gas chromatography/mass spectrometry (GC/MS). Theoretical calculations were carried out on the Gaussian 03 program by using the density functional theory method at the B3LYP/6−311+G(2d,p) level.

Results: The derivatives of three isomeric cresols and six isomeric xylenols have been completely separated on an HP-5MS capillary column within a GC run of only 10 mins. In addition, the derivative of *o*-cresol can be very easily differentiated from its isomers due to its characteristic base peak ion at *m/z* 91 in EI-MS. DFT calculation results indicated that formation of the abundant fragment ion at *m/z* 91 is attributed to a facile dissociation pathway involving the shift of a neighboring phenylmethyl H atom in EI-MS of trimethyl(*o*-tolyloxy)silane.

Conclusions: Silylation provides a promising solution for simultaneous determination of isomeric isomeric cresols and isomeric xylenols.

Keywords: cresol, GC-MS, silylation, isomeric differentiation, DFT

1. Introduction

Phenols have extensively used as raw materials for manufacturing plastics, dyes, pesticides, pharmaceuticals, and other industrial chemicals. Meanwhile, some volatile phenols have been confirmed as biotoxic compounds with teratogenesis, mutagenesis and carcinogenic effect [1,2]. To protect the environment and human oneself, several volatile phenols, including *m*-cresol and 2,4-xylenol, are listed as the priority controlled contamination in many countries. For now, gas chromatography-mass spectrometry is the first choice for determination of these volatile phenols [3-8]. However, *m*-cresol / *p*-cresol and 2,4-xylenol / 2,6-xylenol cannot easily be separated each other on a commercial available GC column [4, 6]. What's worse, these isomers exhibit the nearly identical electron ionization mass spectra. Thus, it is very challenging to accurately determine these isomers at the same time.

Derivatization has been verified as a much effective pre-treatment method in analytical chemistry, which provides a promising strategy for solution of many analytical problems [9,10]. Silylation is an effective characteristic derivatization method for alcohols and phenols, which has been used to improve analytes' thermal stability, volatility and detection sensitivity [11,12]. Several isomeric chlorophenols have been simultaneously determined by silylation and GC-MS analysis [5,6,13]. Silylation has also been used for differentiation of cucurbic acid and its 6,7-stereoisomers by EI-MS [14]. In this work, we try to differentiate these challenging isomeric cresols and isomeric xylenols by silylation and GC-MS.

2. Experimental

2.1 Reagents and Sample Preparation

The analytical reagents of cresols and xylenols were purchased from Aladdin (Beijing, China). MSTFA was purchased from TCI (Japan). Methanol (HPLC-grade) was purchased from Sigma-Aldrich (St Louis, MO, USA), and water (HPLC-grade) was generated using a Milli-Q system (Millipore, Bedford, MA, USA).

2.2 Derivatization

Silylation of cresols was carried out by a classical method (Scheme 1) [12]. Every cresol was mixed with MSTFA in dichloromethane, and the resulting mixture was kept at 40 °C for 30 min. The resulting mixture was directly analyzed by GC-MS or GC-MS/MS.

2.3 GC-MS analysis

The GC-MS experiments were performed using a Trace 2000 GC/DSQ MS instrument (Thermo-Fisher Scientific, Waltham, MA, USA) equipped with an HP-5ms capillary column (30 m long, 0.25 mm id, 0.25 μm film thickness; Agilent Technologies, Santa Clara, CA, USA). Helium (>99.999%) was used as the carrier gas at a constant flow of 1.0 mL min^{-1}. The column temperature was maintained at 80 ºC for 2 min, programmed at 3 ºC min^{-1} to 110 ºC, and then programmed at 25 ºC min^{-1} to 260 ºC, which was maintained for 5 min. The GC inlet temperature was 260 ºC and the transfer line temperature was 250 ºC. Mass spectra were acquired by EI-MS under normal conditions: the ion-source temperature was 200 ºC, the electron energy was 70 eV, the scan rate was 2 scans s^{-1}, and the mass range was 33-600 amu. Xcalibur software (Version 1.4) was used to control the GC-MS instrument and to acquire and process the data.

The GC-MS/MS experiments were performed on a Shimadzu GCMS-TQ8040 instrument (Shimadzu, Japan) equipped with a DB-5ms capillary column (30 m long, 0.25 mm id, 0.25 μm film thickness). The parameters of the GC were similar to the GC-MS experiments. The parameters of MS/MS experiments were set as the following: the

ion-source temperature was 220 °C, the collision energy was 10 eV, and the voltage of the detector was 1.1 kV.

2.4 Theoretical calculations

Theoretical calculations were carried out on the Gaussian 03 program by using the density functional theory (DFT) method at the B3LYP/6-311+G(2d,p) level [15]. The optimized structures for precursor ions, intermediates and products were identified as a true minimum in energy by the absence of imaginary frequencies. The optimized structures were shown by Gauss View (Version 3.09) software. The energies discussed here were the sum of electronic and thermal free energy. The optimized geometry data were available in the supplementary data.

3. Results and Discussion

3.1 GC separation

Fig. 1-a shows the total ion current chromatogram (TIC) of the three isomeric cresols, but only two peaks are observed on the TIC. The peak at t_R 6.13 min corresponds to *o*-cresol by comparison with the retention time of its standard, while *m*- and *p*-cresols co-elute at t_R 6.51 min on the TIC. Thus, it fails to accurately determine *m*-cresol, a precedent-controlled pollutant, at conventional conditions, which might give rise to the false-positive result in analysis of the real samples [4,6]. Similarly, it is also very difficult to separate the priority controlled 2,4-xylenol from 2,6-xylenol on a common chromatographic column. Silylation is a widely-used derivatization method for determination of alcohols and phenols [11,12]. Fortunately, the silylation products of the three isomeric cresols are completely separated on a common HP-5MS capillary column under the conventional condition (Fig. 1-b). The three components at t_R 6.34 min, t_R 6.60 min and t_R 6.74 min in the TIC are corresponding to the silylation derivatives of *o*-, *m*- and *p*- cresols, respectively. Furthermore, a complete separation of the derivatives of three isomeric cresols and six isomeric xylenols has been achieved within a GC run of only 10 mins. A complete chromatographic separation on a commercial available chromatographic column brings a bright prospect for accurate

determination of the three isomeric cresols and six isomeric xylenols.

3.2 EI-MS analysis

Further EI-MS analysis of the three silylation derivatives has been carried out for isomeric differentiation. As shown in Fig. 2, fragmentation of the trimethyl (*o*-tolyloxy)silane radical ion (**M**$^{+\cdot}$, *m/z* 180) mainly produces the dimethyl (methylphenolic)silyl cation (**I165**, *m/z* 165) in path-1, and **I165** undergoes further dissociation to yield the fragment ions of **I149** (*m/z* 149), **I135** (*m/z* 135) and **I91** (*m/z* 91), through the loss of CH_4, C_2H_6, and $O{=}Si(CH_3)_2$, respectively. The above fragmentation pathways have been witnessed by MS/MS analysis of the ion **I165** (See the supplementary Figure S1). Alternatively, breakage of the O-C bond in **M**$^{+\cdot}$ leads to methylphenyl cation (**I91,** *m/z* 91) in path-2. These proposed fragmentation pathways are given in Scheme 2.

To our interest, silylation derivative of *o*-cresol can be easily differentiated from that of the other two isomeric cresols by EI-MS analysis, and the corresponding MS data are summarized in the supplementary Table S1. The fragment ion at *m/z* 165 is the base peak ion in the EI-MS of trimethyl(*m*-tolyloxy)silane and trimethyl(*p*-tolyloxy)silane. Whereas, the ion at *m/z* 91 (100%) rather than the ion at *m/z* 165 (87.5%) becomes the base peak ion in the EI-MS of the *ortho*- isomer, which is distinctively higher in the relative abundance than the corresponding ***m*I91** (*m/z* 91, 28.1%) and ***p*I91** (*m/z* 91, 27.1%). In addition, the product ions of ***o*I149** (*m/z* 149, 17.1%) and ***o*I-135** (*m/z* 135, 56.9%), originating from dissociation of ***o*I165**, are also much more abundant than the corresponding ***m*I149** (*m/z* 149, 6.9%) and ***m*I135** (*m/z* 135, 9.2%), or ***p*I-149** (*m/z* 149, 6.5%) and ***p*I135** (*m/z* 135, 9.5%), respectively. The above results have also been supported by the MS/MS of the ion **I-165** from the three isomeric molecular ions (See the supplementary Figure S2), indicating that ***o*I165** is more feasible to undergo dissociation than ***m*I165** and ***p*I165**. The more instability of ***o*I165** in EI mass spectrum can be explained as the result of the *ortho*-effect [16-19] (Scheme 3), in which a neighboring phenylmethyl H atom participates in the fragmentation pathways and thus promotes these reactions.

3.3 DFT calculation

To further probe the mechanistic *ortho*-effect in EI-MS of the three isomers [16-19], DFT calculations were carried out at the ub3lyp/6-311+g(2d,p) level, and the calculated results were summarized in the supplementary Table S2 and Table 1.

As expected, the lone pair electron on the O atom in the structure of the derivatives is the most preferred to be ionized upon electron impact ionization. Due to the hyper conjugation effect of the methyl moiety, the radical cation ***p*M**$^{+\cdot}$ is located at 12.4 kJ/mol below the *meta*-isomer ***m*M**$^{+\cdot}$ in free energy. Whereas, no significant difference in free energy change (Table 1) was obtained for the fragmentation channels among the *meta*- and the *para*- isomers. Thus, there is no distinctive difference in EI-MS between the *meta*- and the *para*-isomers (Figure 2).

As for the *ortho*- isomer, another fragmentation channels (path-1d1 and path-3 in Scheme 3) was proposed to be responsible for the distinctively high abundance for the ion at *m/z* 91. Optimized structures involved in fragmentation of ***o*M** are shown in Figure 3. Due to the suitable steric conformation, one of the neighboring phenylmethyl hydrogen atoms of ***o*I165** can be easily transferred to the Si atom in the form of hydride in path-1d1 [20-23], which results in an isomeric ion ***o*I165b**. This process needs to overcome an energy barrier of 84.6 kJ/mol (***o*I165-TS**), and the formed ***o*I165b** is located at 34.1 kJ/mol above ***o*I165**. The subsequent elimination of dimethylsilicone from ***o*I165b** results in the benzyl ion (***o*I91b**) at *m/z* 91 *via* migration of the H atom from Si atom the *ipso* carbon on the phenyl ring. This is the key step in the fragmentation pathway with the accumulated energy barrier of 362.8 kJ/mol (***o*I165b-TS**) relative to ***o*M**, which is also 41.9 kJ/mol lower in free energy than the products (***o*I91** and the trimethylsiloxy radical) of path-2, indicating a more feasible dissociation pathway due to the participation of a neighboring phenylmethyl H atom in the fragmentation processes.

Alternatively, in the fragmentation pathway of path-3, one of the neighboring phenylmethyl H atom can be directly transferred to the O atom in the molecular ion ***o*M** through a five-membered ring, which overcomes an energy barrier of 180.1 kJ/mol (***o*M-TS**) and leads to an isomeric radical ion ***o*M2**. The subsequent 1,2-H transfer in ***o*M2** *via* the transition state of ***o*M2-TS** results in another isomeric radical ion ***o*M3**, which is located at

39.5 kJ/mol above ***o*M2**. Then, ***o*M3** undergoes dissociation to give ***o*I91b** at *m/z* 91 by the loss of trimethylsiloxy radical. Overall, the 1,2-H transfer via ***o*M2-TS** is the key step in path-3, with the accumulated energy barrier of 288.0 kJ/mol.

As shown in Table 1, formation of the product ion at *m/z* 91 (**I91**) in path-2 is endoenergic by 413.6 kJ/mol for ***o*M**, 451.6 kJ/mol for ***m*M** and 471.4 kJ/mol for ***p*M**, respectively. By contrast, the accumulated energy barrier for the fragmentation pathway to the product ion at *m/z* 91 (***o*I91-b**) is only 362.8 kJ/mol (***o*I165b-TS**) in path-1d1 and only 288.0 kJ/mol in path-3, respectively. As can be seen, both path-3 and path-1d1 are kinetically more feasible than fragmentation of ***o*M** (***m*M** or ***p*M**) in path-2. Both path-3 and path-1d1 are unique dissociation pathways to the *ortho*- isomer, and thus the *ortho*-isomer has the significantly more abundant fragment ion at *m/z* 91 (base peak) than the other two isomers in EI-MS.

In addition, due to the *ortho* effect, dissociation of the ***o*M** can lead to a more stable fragment ion of ***o*I135b** with a *penta*- cyclic ring in structure (Scheme 3), which is 99.9 kJ/mol lower in free energy than the corresponding ***o*I135** (Table 1). Thus, the product ion at *m/z* 135 (56.9%) in EI-MS of ***o*M** is also much more abundant than the corresponding ***m*I-135** (*m/z* 135, 9.2%), or ***p*I-135** (*m/z* 135, 9.5%). Similar result was obtained for the fragment ion at *m/z* 149 (Table 1).

4. Conclusion

In this work, three isomeric cresols and six isomeric xylenols were differentiated from one another by silylation in combination with GC/MS analysis. These cresols and xylenols were easily converted into the corresponding trimethyl(tolyloxy)silane or (dimethylphenoxy)trimethylsilane, and these derivatives were completely separated on a common HP-5MS capillary column within a GC run of only 10 mins. In addition, the silylation derivative of *o*-cresol can be very easily differentiated from its isomers due to its significantly abundant fragment ions at *m/z* 91, *m/z* 135 and *m/z* 149. DFT calculation results indicated that formation of these abundant fragment ions is attributed to the *ortho* effect in the EI-MS, in which a neighboring phenylmethyl H atom participates in the fragmentation

processes for the *o*- isomer. These results provided a promising solution for simultaneous determination of isomeric cresols and xylenols, and further works in this field will be carried out.

Acknowledgments:

The authors gratefully acknowledge financial support from Scientific Research Projects of Zhejiang Education Department (No.Y201533091), the Natural Science Foundation of Zhejiang Province (No. LQ17E030001). Computer time was made available on the SGI Aktix 450 sever at Computational Center for Molecular Design of Organosilicon Compounds, Hangzhou Normal University.

Reference:

1. R. Shoji, M. Kawakami. Prediction of genotoxicity of various environmental pollutants by artificial neural network simulation. *Mol. Div.* **2006**, *10*, 101.
2. H. H. Lo, I. P. Brown, O. G. Rankin. Acute nephrotoxicity induced by isomeric dichloroanilines in fischer 344 rats. *Toxicol.* **1990**, *63*, 215.
3. C. Li, F. Jin, S.A. Snyder. Recent advancements and future trends in analysis of nonylphenol ethoxylates and their degradation product nonylphenol in food and environment. *TrAC Trend. Anal. Chem.* **2018**, *107*, 78.
4. J. Peng, Y. Zhang, X. Yang, M. Qi. High-resolution separation performance of poly-(caprolactone)diol for challenging isomers of xylenes, phenols and anilines by capillary gas chromatography. *J. Chromatogr. A.* **2016**, *1466*, 148.
5. Á.g. Kovács, M.r. Mörtl, A. Kende. Development and optimization of a method for the analysis of phenols and chlorophenols from aqueous samples by gas chromatography-mass spectrometry, after solid-phase extraction and trimethylsilylation. *Microchem. J.* **2011**, *99*, 125.
6. Á.g. Kovács, A. Kende, M.r. Mörtl, G.b. Volk, T.s. Rikker, K.l. Torkos. Determination of phenols and chlorophenols as trimethylsilyl derivatives using gas chromatography-mass spectrometry. *J. Chromatogr. A.* **2008**, *1194*, 139.
7. R. Baciocchi, M. AttinÃ, G. Lombardi, M.R. Boni. Fast determination of phenols in contaminated soils. *J. Chromatogr. A.* **2001**, *911*, 135.
8. L. Wennrich, P. Popp, M. Möder. Determination of chlorophenols in soils using accelerated solvent extraction combined with solid-phase microextraction. *Anal. Chem.* **2000**, *72*, 546.
9. B.-L. Qi, P. Liu, Q.-Y. Wang, W.-J. Cai, B.-F. Yuan, Y.-Q. Feng. Derivatization for liquid

chromatography-mass spectrometry. *TrAC Trends Anal. Chem.* **2014**, *59*, 121.
10. Y. Wu, L. Li. Dansylation metabolite assay: A simple and rapid method for sample amount normalization in metabolomics. *Anal. Chem.***2014**, *86*, 9428.
11. T. Nishikaze, H. Tsumoto, S. Sekiya, S. Iwamoto, Y. Miura, K. Tanaka. Differentiation of sialyl linkage isomers by one-pot sialic acid derivatization for mass spectrometry-based glycan profiling. *Anal. Chem.* **2017**, *89*, 2353.
12. J. Halket, V. Zaikin. Derivatization in mass spectrometry-1. Silylation. *Eur. J. Mass Spectrom*. **2003**, *9*, 1.
13. M. Saraji, H. Ghambari. Suitability of dispersive liquid–liquid microextraction for the in situ silylation of chlorophenols in water samples before gas chromatography with mass spectrometry. *J. Sep. Sci*. **2015**, *38*, 3552.
14. J.-F. Rontani, M.-A. Galeron, C. Aubert. Electron ionization mass spectrometric fragmentation and multiple reaction monitoring quantification of trimethylsilyl derivatives of cucurbic acid and its 6,7-stereoisomers. *Rapid Commun. Mass Spectrom*. **2016**, *30*, 2253.
15. M. J. Frisch, G. W. Trucks, H. B. Schlegel, G. E. Scuseria, M. A. Robb, J. R. Cheeseman, V. G. Zakrzewski, J. A. Montgomery, Jr, R. E. Stratmann, J. C. Burant, S. Dapprich, J. M. Millam, A. D. Daniels, K. N. Kudin, M. C. Strain, O. Farkas, J. Tomasi, V. Barone, M. Cossi, R. Cammi, B. Mennucci, C. Pomelli, C. Adamo, S. Clifford, J. Ochterski, G. A. Petersson, P. Y. Ayala, Q. Cui, K. Morokuma, D. K. Malick, A. D. Rabuck, K. Raghavachari, J. B. Foresman, J Cioslowski, J. V. Ortiz, B. B. Stefanov, G. Liu, A. Liashenko, P. Piskorz, I. Komaromi, R. GomPerts, R. L. Martin, D. J. Fox, T. Keith, M. A. Al-Laham, C. Y. Peng, A. Nanayakkara, C. Gonzalez, M. Challacombe, P. M. W. Gill, B. Johnson, W. Chen, M. W. Wong, J. L. Andres, C. Gonzalez, M. E. Head-Gordon, S. Replogle, J. A. Pople. *Gaussian 03*, Inc. Pittsburgh PA. **2003**.
16. F.B. Jariwala, M. Figus, A.B. Attygalle. Ortho effect in electron ionization mass spectrometry of *N*-acylanilines bearing a proximal halo substituent. *J. Am. Soc. Mass Spectrom*. **2008**, *19*, 1114.
17. M. Mendes, R. Rittner, M. Eberlin, J. Suwinski, W. Szczepankiewicz. Ortho effects in the dissociation of ionized N-chlorophenyl- and N-bromophenyl-2-aminobenzamidines: Intramolecular aromatic substitution with cyclization to protonated 2-(2-aminophenyl)-1H-benzimidazoles. *Eur. J. Mass Spectrom.* **2002**, *8*, 27.
18. D. Błachut, W. Danikiewicz, M. Olejnik, Z. Czarnocki. Electron ionization mass spectrometry as a tool for the investigation of the ortho effect in fragmentation of some Schiff bases derived from amphetamine analogs. *J. Mass Spectrom.* **2004**, *39*, 966.
19. K. Jiang, G. Bian, Y. Pan, G. Lai. Recognizing ortho-, meta- or para-positional isomers of S-methyl methoxylphenylmethylenehydrazine dithiocarboxylates by ESI-MS^2: the positional effect of the methoxyl substituent. *Int. J. Mass Spectrom*. **2011**, *299*, 13.
20. Y. Chai, K. Jiang, Y. Pan. Hydride transfer reactions via ion–neutral complex: fragmentation of protonated *N*-benzylpiperidines and protonated *N*-benzyl piperazines in

mass spectrometry. *J. Mass. Spectrom.* **2010**, *45*, 496.
21. Y. Chai, L. Wang, H. Sun, C. Guo, Y. Pan. Gas-Phase Chemistry of Benzyl Cations in Dissociation of *N*-Benzylammonium and *N*-Benzyliminium Ions Studied by Mass Spectrometry. *J. Am. Soc. Mass Spectrom*. **2012**, *23*,823.
22. F. Li, X. Zhang, H. Zhang, K. Jiang. Gas-phase fragmentation of the protonated benzyl ester of proline: intramolecular electrophilic substitution versus hydride transfer. *J. Mass Spectrom.* **2013**, *48*, 423.

Table 1. Free energy (Hartree) and relative free energy (kJ/mol) of the key species in fragmentation of the trimethyl(*o*-tolyloxy)silane radical ions.

Structure	***Rel G (kJ/mol)***		
	ortho-	***meta-***	***para-***
$M^{+\cdot}$	8.9	12.4	0.0*
I-165 + $\cdot CH_3$	168.8	159.7	163.3
I149 + $\cdot CH_3$ + CH_4	468.4	468.5	469.1
I149b + $\cdot CH_3$ + CH_4	177.5	-	-
I135 + $\cdot CH_3$ + C_2H_6	379.9	374.3	385.2
I135b + $\cdot CH_3$ + CH_4	280.0	-	-
I91 + $Me_3SiO\cdot$	413.6	464.0	471.4

* Relative free energy (kJ/mol) of ***p*M$^{+\cdot}$** was set at zero.

Scheme 1. Silylation of cresol

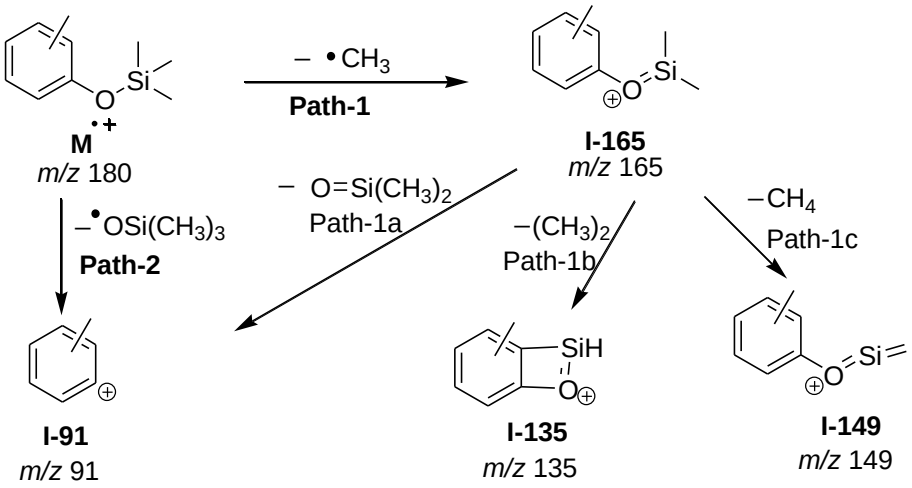

Scheme 2. The proposed fragmentation pathways of trimethyl(tolyloxy)silane radical ion

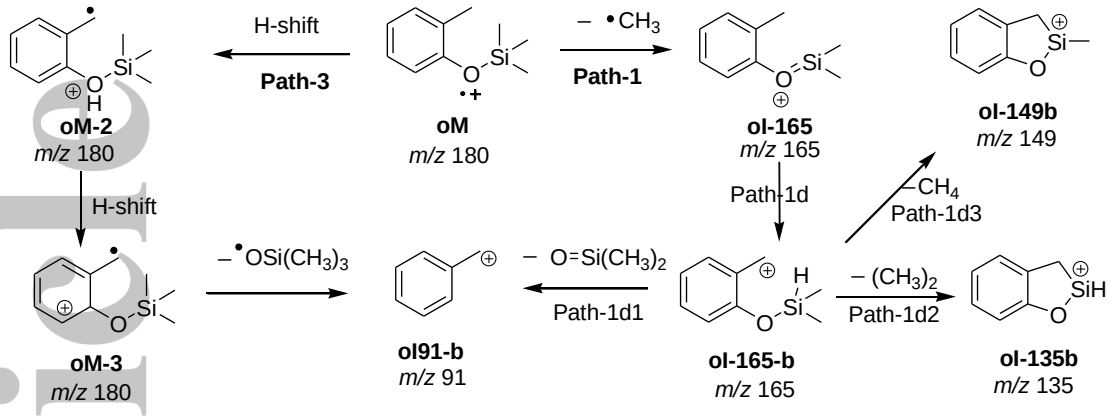

Scheme 3. The proposed fragmentation pathways of trimethyl(*o*-tolyloxy)silane radical ion

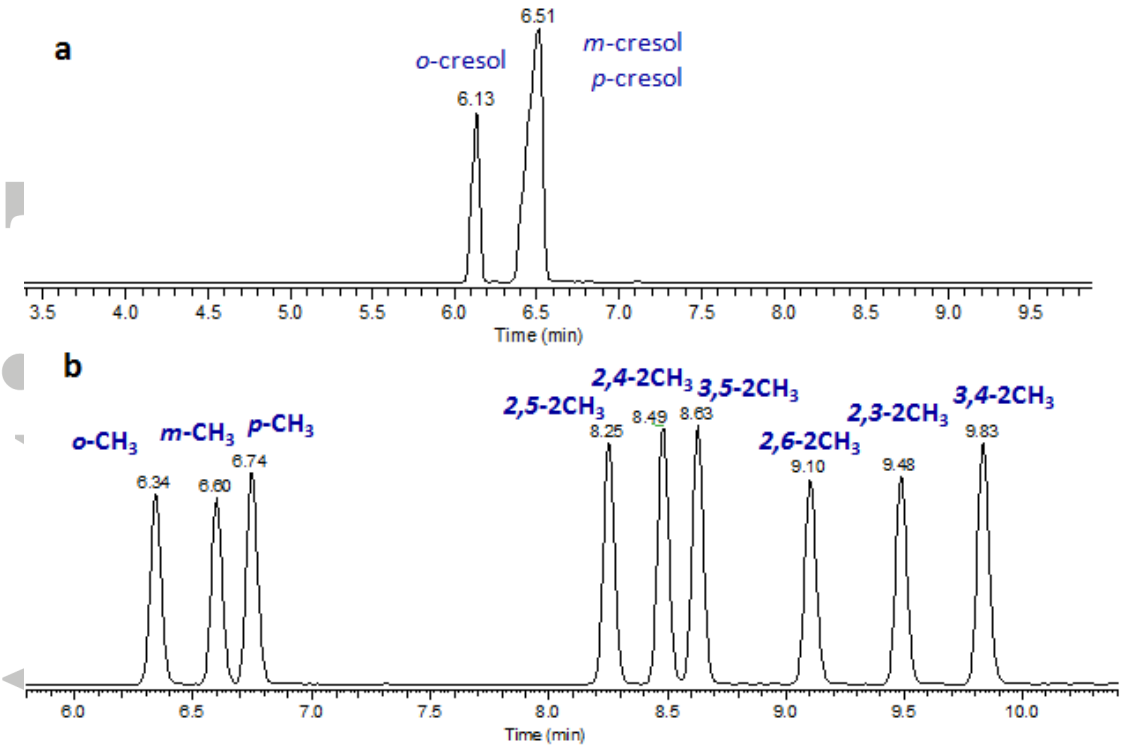

Figure. 1 TIC of isomeric cresols (a) and the silylation derivatives of three isomeric cresols and six xylenols (b)

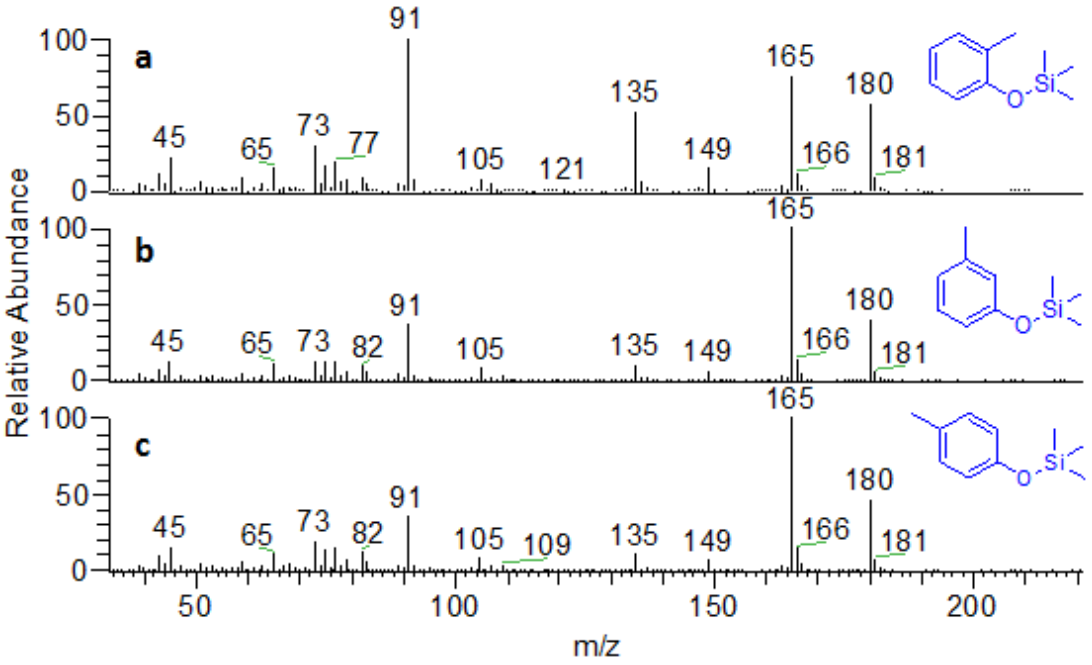

Figure 2. EI-MS of the isomeric trimethyl(*o*-tolyloxy)silanes

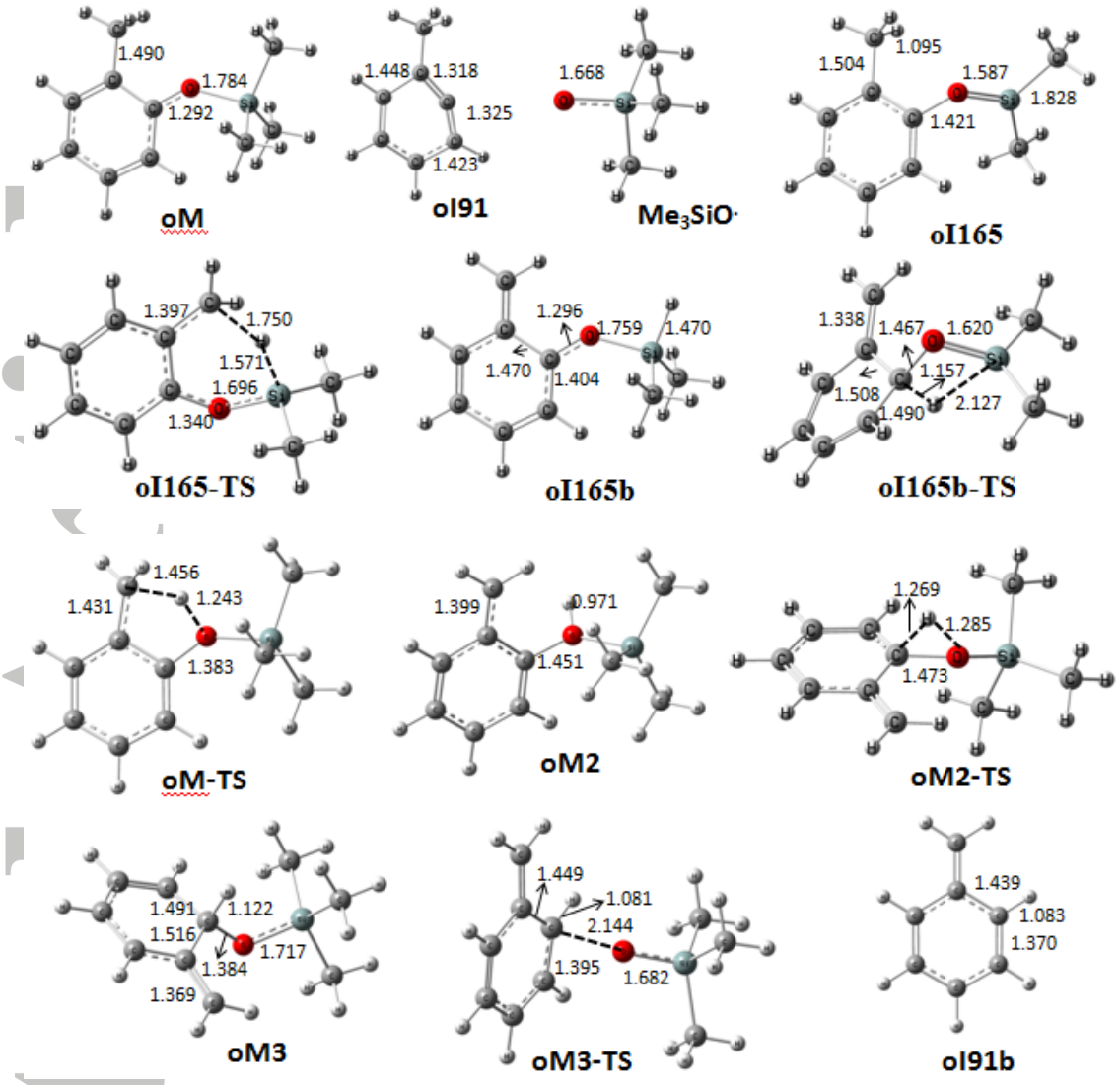

Figure 3. Optimized structures involved in fragmentation of ***o*M**

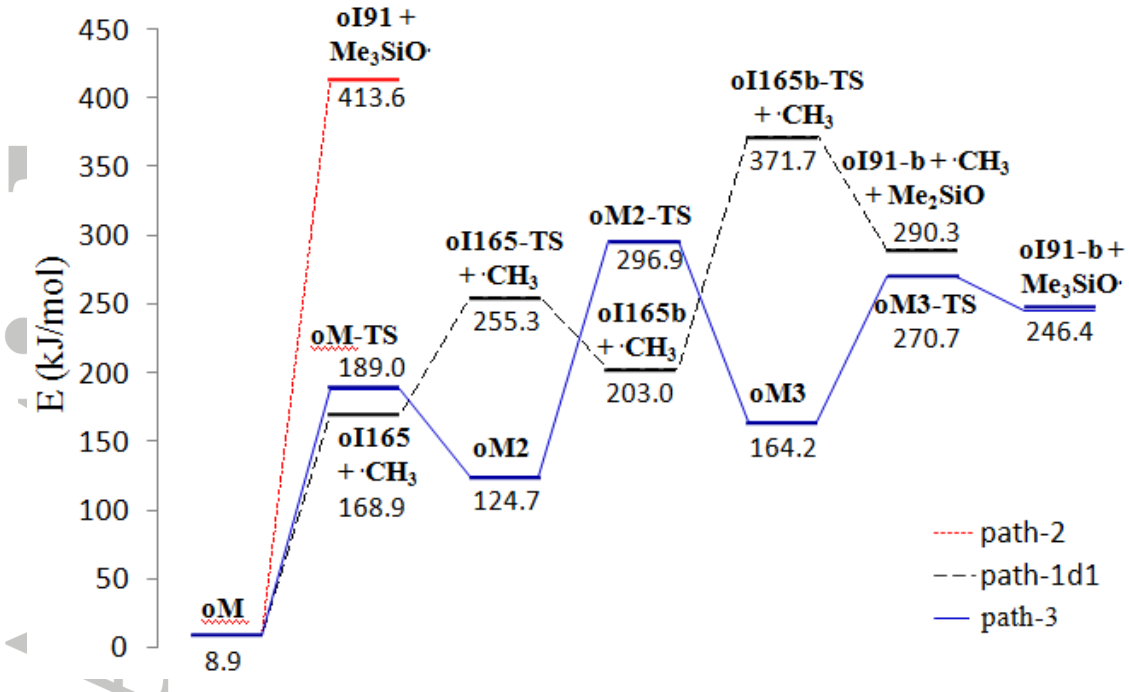

Figure 4. Potential energy diagram for the fragmentation pathways of ***o*-M**$^{+\cdot}$ to the ions at *m/z* 91